

Turbulent Heat Transfer in an Enclosure With a Horizontal Permeable Plate in the Middle

Edimilson J. Braga

Marcelo J. S. de Lemos¹

Mem. ASME

e-mail: delemos@ita.br

Departamento de Energia—IEME,
Instituto Tecnológico de Aeronáutica—ITA,
12228-900, São José dos Campos, SP,
Brazil

Turbulent natural convection in a vertical two-dimensional square cavity, isothermally heated from below and cooled at the upper surface, is numerically analyzed using the finite volume method. The enclosure has a thin horizontal porous obstruction, made of a highly porous material and extremely permeable, located at the cavity midheight. Governing equations are written in terms of primitive variables and are recast into a general form. For empty cavities, no discrepancies result for the Nusselt number when laminar and turbulent model solutions are compared for Rayleigh numbers up to 10^7 . Also, in general the porous obstruction decreases the heat transfer across the heated walls showing overall lower Nusselt numbers when compared with those without the porous obstruction. However, the presence of a porous plate in the cavity seems to force an earlier separation from laminar to turbulence model solutions due to higher generation rates of turbulent kinetic energy into the porous matrix. [DOI: 10.1115/1.2352779]

Keywords: turbulence, porous media, heat transfer, natural convection

1 Introduction

The analysis of buoyancy-driven flows in an enclosed cavity provides useful comparisons for evaluating the robustness and performance of numerical methods dealing with viscous flow calculations. The importance of the enclosure natural-convection phenomena can best be appreciated by noting several of their application areas. Nuclear reactor safety, heat exchangers, underground spread of pollutants, environmental control, grain storage, food processing, material processing, geothermal systems, oil extraction, store of nuclear waste material, solar power collectors, optimal design of furnaces, crystal growth in liquids, and packed-bed catalytic reactors are some examples of applications of heat removal or addition by free convection mechanism.

The study of natural convection in enclosures still attracts the attention of researchers and a significant number of experimental and theoretical works have been carried out mainly from the 1970s. During the conference on Numerical Methods in Thermal Problems, which took place in Swansea, Jones [1] proposed that buoyancy-driven flow in a square cavity would be a suitable vehicle for testing and validating computer codes. Following discussions at Swansea, contributions for the solution of the problem were invited. The compilation and discussion of the main contributions yielded the classical benchmark of Refs. [2,3].

The first to introduce a turbulence model in their calculations were Markatos and Pericleous [4]. They performed steady 2D simulations for Ra up to 10^{16} and presented a complete set of results. The work of Henkes, van der Vlugt, and Hoogendoorn [5] used the same turbulence model adopted by Markatos and Pericleous [4] for 2D calculations up to Ra= 10^{11} . In Ref. [5] 2D calculations using various versions of the k - ϵ turbulence model was performed. These versions included the standard as well as the low-Reynolds number k - ϵ models. A comparison with experimental results for Nu showed the superiority of the low-Reynolds number k - ϵ closures. In Ref. [6], 3D calculations for laminar flow

for Ra up to 10^{10} were presented. Their graphs revealed the 3D character of the flow. Comparisons were made with 2D simulations and differences were reported for the heat transfer correlation between Nu and Ra. A recent paper by Barakos, Mitsoulis, and Assimacopoulos [7] reworked the problem for laminar and turbulent flows for a wide range of Ra. Turbulence was modeled with the standard k - ϵ closure and the effect of wall functions on heat transfer was investigated.

Studies concerning natural convection in porous media can be found in the monographs of Refs. [8,9]. The case of free convection in a rectangular cavity heated on a side and cooled at the opposing side is also an important problem in thermal convection in porous media. The works of Walker and Homsy [10], Bejan [11], Prasad and Kulacki [12], Beckermann, Viskanta, and Ramadhyani [13], Gross, Bear, and Hickox [14], and Manole and Lage [15] have contributed with some important results to this problem. The recent work of Baytas and Pop [16] was concerned with a numerical study of the steady free convection flow in rectangular and oblique cavities filled with homogeneous porous media using a nonlinear axis transformation. The Darcy momentum and energy equations are solved numerically using the (ADI) method.

Studies on macroscopic transport modeling of incompressible flows in porous media have been based on the volume-average methodology for either heat [17] or mass transfer [18–20]. In turbulent flows, when time fluctuations of the flow properties are also considered in addition to spatial deviations, there are two possible methodologies to follow in order to obtain macroscopic equations: (a) application of time-average operator followed by volume averaging [21–24], or (b) use of volume-averaging before time-averaging is applied [25–27]. However, both sets of macroscopic mass transport equations are equivalent when examined under the recently established *double decomposition concept* [28–31]. This theoretical work has been extended to heat transfer in porous media where both time fluctuations and spatial deviations were considered for temperature and velocity [32,33]. Further, a consistent program of systematic analyzes based on the *double-decomposition theory* for treating turbulent buoyant flows [34,35], nonequilibrium heat transfer [36,37], mass transfer [38], and double diffusion [39], has been applied to investigate flow through porous inserts [40], heat transfer in permeable baffles [41], and flow over a finite porous substrate considering a diffusion-

¹Corresponding author.

Contributed by the Heat Transfer Division of ASME for publication in the JOURNAL OF HEAT TRANSFER. Manuscript received April 15, 2005; final manuscript received April 5, 2006. Review conducted by N. K. Anand. Paper presented at the 2003 ASME International Mechanical Engineering Congress (IMECE2003), November 15–21, 2003, Washington, D.C.

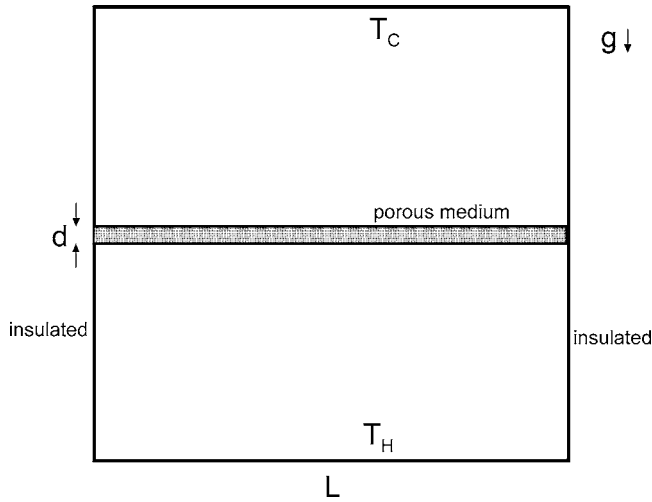


Fig. 1 Geometry under consideration

jump condition at the interface for the mean [42,43] and turbulence fields [44,45]. All those studies were based on the concepts first proposed by [28–31], which were compared to other views the literature in [46]. Recently, a book has been published on the subject of turbulence modeling in porous media [47].

Motivated by the foregoing work, this work presents turbulent natural convection in a vertical two-dimensional square cavity, isothermally heated from below and cooled at the upper surface. The enclosure has a thin horizontal porous obstruction located at the cavity mid height. As the overall heat flux across the enclosure is from bottom to top, this geometry is here considered a vertical. The turbulence model here adopted is the standard k - ϵ with wall function.

2 The Problem Considered

The problem considered is shown schematically in Fig. 1 and refers to the two-dimensional flow of a Boussinesq fluid of Prandtl number 1 in a square cavity of side $L=1$ m. The cavity is assumed to be of infinite depth along the z -axis and is isothermally heated from the bottom and cooled from the ceiling. The vertical square cavity has a porous obstruction of thickness $d=0.05$ m positioned at cavity midheight.

The no-slip condition is applied for velocity and the resulting flow is treated as steady. The controlling parameter is the Rayleigh number, $Ra=g\beta H^3\Delta T/\nu\alpha$, which was varied up to 10^7 only to ensure that for unobstructed cavities the flow is practically laminar. Further, a relationship for the permeability was proposed in Refs. [46,48] for circular rods, which are in good accord with the empirical expression proposed by Ref. [49], as:

$$K = \frac{D_p^2 \phi^3}{144(1-\phi)^2} \quad (1)$$

3 Governing Equations

The equations used herein are derived in details in the work of Refs. [29,32,33,35]. Basically, for porous media analysis, a macroscopic form of the governing equations is obtained by taking the volumetric average of the entire equation set. In that development, the porous medium is considered to be rigid and saturated by an incompressible fluid.

The macroscopic continuity equation is given by,

$$\nabla \cdot \bar{\mathbf{u}}_D = 0 \quad (2)$$

The Dupuit–Forchheimer relationship, $\bar{\mathbf{u}}_D = \phi \langle \bar{\mathbf{u}} \rangle^i$, has been used and $\langle \bar{\mathbf{u}} \rangle^i$ identifies the intrinsic (liquid) average of the local

velocity vector $\bar{\mathbf{u}}$. The macroscopic time-mean Navier–Stokes (NS) equation for an incompressible fluid with constant properties is given as

$$\rho \left[\frac{\partial \bar{\mathbf{u}}_D}{\partial t} + \nabla \cdot \left(\frac{\bar{\mathbf{u}}_D \bar{\mathbf{u}}_D}{\phi} \right) \right] = -\nabla(\phi \langle \bar{p} \rangle^i) + \mu \nabla^2 \bar{\mathbf{u}}_D + \nabla \cdot (-\rho \phi \langle \bar{\mathbf{u}}' \bar{\mathbf{u}}' \rangle^i) - \rho \beta_\phi \mathbf{g} \phi (\langle \bar{T} \rangle^i - T_{ref}) - \left[\frac{\mu \phi}{K} \bar{\mathbf{u}}_D + \frac{c_F \phi \rho |\bar{\mathbf{u}}_D| \bar{\mathbf{u}}_D}{\sqrt{K}} \right] \quad (3)$$

The use of Eq. (3) is largely employed in the literature when “numerical” solutions are sought for a “macroscopic” view of the flow. As such, Eq. (3) is used when one seeks modeling the “overall” effect of the porous substrate on the flow. The interested reader is referred to Refs. [28–31] for extensive discussions on this important point.

Further, when treating turbulence with statistical tools, the correlation $-\rho \bar{\mathbf{u}}' \bar{\mathbf{u}}'$ appears after application of the time-average operator to the local instantaneous NS equation. Applying further the volume-average procedure to this correlation results in the term $-\rho \phi \langle \bar{\mathbf{u}}' \bar{\mathbf{u}}' \rangle^i$. This term is here recalled the macroscopic Reynolds stress tensor (MRST). Further, a model for the MRST in analogy with the Boussinesq concept for clear fluid can be written as

$$-\rho \phi \langle \bar{\mathbf{u}}' \bar{\mathbf{u}}' \rangle^i = \mu_{i,\phi} 2 \langle \bar{\mathbf{D}} \rangle^v - \frac{2}{3} \phi \rho \langle k \rangle^i \mathbf{I} \quad (4)$$

where

$$\langle \bar{\mathbf{D}} \rangle^v = \frac{1}{2} [\nabla(\phi \langle \bar{\mathbf{u}} \rangle^i) + [\nabla(\phi \langle \bar{\mathbf{u}} \rangle^i)]^T] \quad (5)$$

is the macroscopic deformation rate tensor, $\langle k \rangle^i$ is the intrinsic average for k and $\mu_{i,\phi}$ is the macroscopic turbulent viscosity. The macroscopic turbulent viscosity, $\mu_{i,\phi}$, is modeled similarly to the case of clear fluid flow and a proposal for it was presented in Ref. [29] as

$$\mu_{i,\phi} = \rho c_\mu \frac{\langle k \rangle^i{}^2}{\langle \epsilon \rangle^i} \quad (6)$$

In a similar way, applying both time and volumetric average to the microscopic energy equation, for either the fluid or the porous matrix, two equations arise. Assuming further the local thermal equilibrium hypothesis, which considers $\langle \bar{T}_f \rangle^i = \langle \bar{T}_s \rangle^i = \langle \bar{T} \rangle^i$, and adding up these two equations, one has

$$(\rho c_p)_f \nabla \cdot (\phi \langle \bar{\mathbf{u}} T_f \rangle^i) = (\rho c_p)_f \nabla \cdot \left\{ \begin{array}{l} \text{I} \quad \phi \langle \langle \bar{\mathbf{u}} \rangle^i \langle \bar{T}_f \rangle^i \rangle \\ \text{II} \quad \langle \bar{\mathbf{u}}' \rangle^i \langle \bar{T}_f' \rangle^i \\ \text{III} \quad \langle \bar{\mathbf{u}}' \bar{T}_f \rangle^i \\ \text{IV} \quad \langle \bar{\mathbf{u}}' \bar{T}_f' \rangle^i \end{array} \right\} \quad (7)$$

where to each term on the right hand side of Eq. (7), the following significance can be attributed: I convection—due to macroscopic time-averaged velocity and temperature, II turbulent heat flux—due to the macroscopic time fluctuations of local velocity and temperature, III thermal dispersion—associated with spatial deviations of the time averaged velocity and temperature. Note that this term is also present in laminar flows in porous media. IV turbulent thermal dispersion—due to both time fluctuations and spatial deviations of local velocity and temperature.

A modeled form of Eq. (7) has been given in detail in the work of Rocamora, Jr. and de Lemos [32,33], as

$$\{(\rho c_p)_f \phi + (\rho c_p)_s (1-\phi)\} \frac{\partial \langle \bar{T} \rangle^i}{\partial t} + (\rho c_p)_f \nabla \cdot (\mathbf{u}_D \langle \bar{T} \rangle^i) = \nabla \cdot \{ \mathbf{K}_{eff} \cdot \nabla \langle \bar{T} \rangle^i \} \quad (8)$$

where, \mathbf{K}_{eff} , given by

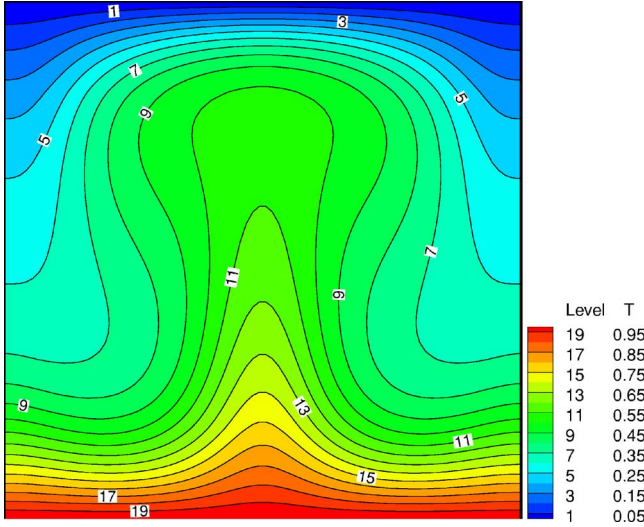


Fig. 2 Isotherms for laminar solution for a square cavity heated from below and cooled from the ceiling for $Ra=4 \times 10^4$

$$\mathbf{K}_{\text{eff}} = [\phi k_f + (1 - \phi)k_s] \mathbf{I} + \mathbf{K}_{\text{tor}} + \mathbf{K}_t + \mathbf{K}_{\text{disp}} + \mathbf{K}_{\text{disp},t} \quad (9)$$

is the effective conductivity tensor. In order to be able to apply (8), it is necessary to determine the conductivity tensors in (9), i.e., \mathbf{K}_{tor} , \mathbf{K}_t , \mathbf{K}_{disp} , and $\mathbf{K}_{\text{disp},t}$. Following Ref. [23], this can be accomplished for the tortuosity and thermal dispersion conductivity tensors, \mathbf{K}_{tor} and \mathbf{K}_{disp} , by making use of a unit cell subjected to periodic boundary conditions for the flow and a linear temperature gradient imposed over the domain. The conductivity tensors are then obtained directly from the microscopic results for the unit cell (see Ref. [23] for details on the expressions here used).

The turbulent heat flux and turbulent thermal dispersion terms, \mathbf{K}_t and $\mathbf{K}_{\text{disp},t}$, which cannot be determined from such a microscopic calculation, are modeled here through the Eddy diffusivity concept, similarly to Ref. [24]. It should be noticed that these terms arise only if the flow is turbulent, whereas the tortuosity and the thermal dispersion terms exist for both laminar and turbulent flow regimes.

Starting out from the time averaged energy equation coupled with the microscopic modeling for the “turbulent heat flux” through the eddy diffusivity concept, one can write, after volume averaging

$$-(\rho c_p)_f \overline{\mathbf{u}' T_f'} = (\rho c_p)_f \frac{\nu_{t,\phi}}{\sigma_T} \nabla \langle \bar{T}_f \rangle^i \quad (10)$$

where the symbol $\nu_{t,\phi}$ expresses the macroscopic eddy viscosity, $\mu_{t,\phi} = \rho_f \nu_{t,\phi}$, given by (6) and σ_T is a constant. According to (10), the macroscopic heat flux due to turbulence is taken as the sum of the turbulent heat flux and the turbulent thermal dispersion found by Ref. [33]. In view of the arguments given above, the turbulent heat flux and turbulent thermal dispersion components of the conductivity tensor, \mathbf{K}_t and $\mathbf{K}_{\text{disp},t}$, respectively, are expressed as

$$\mathbf{K}_t + \mathbf{K}_{\text{disp},t} = \phi (\rho c_p)_f \frac{\nu_{t,\phi}}{\sigma_T} \mathbf{I} \quad (11)$$

In the equation set shown above, when the variable $\phi=1$, the domain is considered as a clear medium. For any other value of ϕ , the domain is treated as a porous medium.

3.1 Nusselt number. The local Nusselt number on the hot wall for the square cavity at $x=0$ is defined as

$$Nu = hH/k : Nu = \left(\frac{\partial \langle T \rangle^v}{\partial y} \right)_{y=0} \frac{H}{T_H - T_C} \quad (12)$$

and the average Nusselt number is given by

$$\bar{Nu} = \frac{1}{L} \int_0^L Nu dx \quad (13)$$

4 Turbulence Model

Transport equations for $\langle k \rangle^i = \overline{\langle \mathbf{u}' \cdot \mathbf{u}' \rangle^i} / 2$ and $\langle \varepsilon \rangle^i = \mu \langle \nabla \mathbf{u}' : (\nabla \mathbf{u}')^T \rangle^i / \rho$ in their so-called high Reynolds number form are proposed in Ref. [29] and extended in Ref. [35] to incorporate the buoyant effects as

$$\rho \left[\frac{\partial}{\partial t} (\phi \langle k \rangle^i) + \nabla \cdot (\bar{\mathbf{u}}_D \langle k \rangle^i) \right] = \nabla \cdot \left[\left(\mu + \frac{\mu_{t,\phi}}{\sigma_k} \right) \nabla (\phi \langle k \rangle^i) \right] + P^i + G^i + G_\beta^i - \rho \phi \langle \varepsilon \rangle^i \quad (14)$$

$$\rho \left[\frac{\partial}{\partial t} (\phi \langle \varepsilon \rangle^i) + \nabla \cdot (\bar{\mathbf{u}}_D \langle \varepsilon \rangle^i) \right] = \nabla \cdot \left[\left(\mu + \frac{\mu_{t,\phi}}{\sigma_\varepsilon} \right) \nabla (\phi \langle \varepsilon \rangle^i) \right] + c_1 P^i \frac{\langle \varepsilon \rangle^i}{\langle k \rangle^i} + c_2 \frac{\langle \varepsilon \rangle^i}{\langle k \rangle^i} G^i + c_1 c_3 G_\beta^i \frac{\langle \varepsilon \rangle^i}{\langle k \rangle^i} - c_2 \rho \phi \frac{\langle \varepsilon \rangle^i{}^2}{\langle k \rangle^i} \quad (15)$$

where c_1 , c_2 , c_3 , and c_k are constants, $P^i = (-\rho \langle \mathbf{u}' \mathbf{u}' \rangle^i : \nabla \bar{\mathbf{u}}_D)$ is the production rate of $\langle k \rangle^i$ due to gradients of $\bar{\mathbf{u}}_D$, $G^i = [c_k \rho (\phi \langle k \rangle^i) |\bar{\mathbf{u}}_D| / \sqrt{K}]$ is the generation rate of the intrinsic average of \mathbf{k} due to the action of the porous matrix and $G_\beta^i = [\phi (\mu_{t,\phi} / \sigma_T) \mathbf{g}_\beta \nabla \langle \bar{T} \rangle^i]$ is the generation rate of $\langle k \rangle^i$ due to the buoyant effects.

Before proceeding, a word about the class of problems under consideration herein seems timely. Cases here investigated are akin to having a forced flow through a grid. The grid, or any “highly permeable” structure, will perturb the flow rather than “suppress” it, inducing instabilities leading eventually to turbulent regime. Evidently, if the flow restriction is intense, then a substantial reduction on the mass flow rate across the porous material is resultant for the same ΔT across the cavity. This, however, is not the situation here. The class of problems treated in this paper deals only with highly permeable, highly porous structure so that no substantial head loss is added to the flow. The source term G^i in Eq. (14) reflects this notion and physically represents an additional generation rate of k due to the flow perturbation caused by the highly permeable obstruction. Comprehensive discussions on this matter are available in Refs. [29–31,46], which are suggested for further reading.

The interface conditions between the clear medium and the porous medium follows the work of Ochoa-Tapia and Whitaker [50] using the “shear stress jump” concept. At the interface one has (see Fig. 1),

$$\bar{\mathbf{u}}_D|_{\phi < 1} = \bar{\mathbf{u}}_D|_{\phi = 1} \quad (16)$$

$$\langle \bar{p} \rangle^i|_{\phi < 1} = \langle \bar{p} \rangle^i|_{\phi = 1} \quad (17)$$

$$\phi^{-1} \frac{\partial \bar{u}_{D1}}{\partial x_2} \Big|_{\phi < 1} - \frac{\partial \bar{u}_{D1}}{\partial x_2} \Big|_{\phi = 1} = \frac{\beta_i}{\sqrt{K}} \bar{u}_{D1} \Big|_{\text{interface}} \quad (18)$$

$$\langle k \rangle^v|_{\phi < 1} = \langle k \rangle^v|_{\phi = 1} \quad (19)$$

$$\left(\mu + \frac{\mu_{t,\phi}}{\sigma_k} \right) \frac{\partial \langle k \rangle^v}{\partial x_2} \Big|_{\phi < 1} = \left(\mu + \frac{\mu_{t,\phi}}{\sigma_k} \right) \frac{\partial \langle k \rangle^v}{\partial x_2} \Big|_{\phi = 1} \quad (20)$$

$$\langle \varepsilon \rangle^v|_{\phi < 1} = \langle \varepsilon \rangle^v|_{\phi = 1} \quad (21)$$

$$\left(\mu + \frac{\mu_t}{\sigma_\varepsilon} \right) \frac{\partial \langle \varepsilon \rangle^v}{\partial x_2} \Big|_{\phi < 1} = \left(\mu + \frac{\mu_t}{\sigma_\varepsilon} \right) \frac{\partial \langle \varepsilon \rangle^v}{\partial x_2} \Big|_{\phi = 1} \quad (22)$$

$$\langle \bar{T} \rangle^i|_{\phi < 1} = \langle \bar{T} \rangle^i|_{\phi = 1} \quad (23)$$

$$\mathbf{e}_2 \cdot (\underline{K}_{\text{eff}} \cdot \nabla \langle \bar{T} \rangle^i)|_{\phi < 1} = k_f \frac{\partial \langle \bar{T} \rangle^i}{\partial x_2} \Big|_{\phi = 1} \quad (24)$$

where β_i in Eq. (18) is a nondimensional coefficient that expresses a “jump” condition in the shear stress at the interface. Such discontinuity might be due to interface roughness or be a way to comply with irregular interfaces. In addition, it can also be seen as an accommodation of the fact that close to the interface the permeability K attains higher values than those used within the porous substrate. The interface conditions for k and ε , Eqs. (19)–(22) were proposed by Ref. [51] and used in Refs. [42–45]. They assume continuity of k and ε at the interface. One should point out, however, that the use of Eq. (18) has very little influence on flows mostly normal to the interface, as in the case here analyzed (see Ref. [40] for flow computations normal to a porous insert). Here, Eq. (18) is considered for the sake of completeness only.

5 Numerical Method and Solution Procedure

The numerical method employed for discretizing the governing equations is the control-volume approach with a generalized collocated grid. The flux blended deferred correction which combines linearly the upwind differencing scheme and central differencing scheme, was used for interpolating the convective fluxes, see Ref. [52]. The well-established SIMPLE algorithm [53] is followed for handling the pressure-velocity coupling. Individual algebraic equation sets were solved by the SIP procedure of (see Refs. [54,55] for details). Further, concentration of nodal points to walls reduces eventual errors due to numerical diffusion which, in turn, are further annihilated due to the hybrid scheme here adopted.

6 Results and Discussion

Calculations for turbulent flow were performed for all cases using an 80×120 grid with concentration of nodes near the horizontal walls. Runs were performed with high porosity, $\phi=0.95$, $k_t/k_f=2$, $\text{Pr}=1$, and an equivalent particle diameter, $D_p=1$ mm (see Eq. (1)), which gives a $\text{Da}=K/L^2=0.2382 \times 10^{-5}$ in order to permit a high mass flux through the porous obstruction and to avoid suppression of convective currents.

It is important to emphasize that the main objective of this work is not to simulate the transition mechanism from laminar regime to fully turbulent flow, which involves modeling of complex physical processes and hydrodynamic instabilities. Here, the aim of this work is to establish when both turbulent and laminar models do not differ substantially as far as predictions of overall Nu are of concern. Therefore, a strategy for determining the range of validity of a laminar flow solution was to simulate the *laminarization* of turbulent flow when the Raleigh number is reduced. Or say, we start with a low value of Ra and the “laminar” model, compute Nu and repeat the calculations for increasing Raleigh numbers. Also, we turn on the k - ε model for $\text{Ra}=10^7$, calculate Nu, and repeat the procedure for smaller Ra’s, remembering that such a two-equation model was first proposed with the aim of predicting the laminarization process. We perform calculations with and without the porous obstruction and compare the behavior of Nu in both cases.

According to Ref. [5], the separation of the averaged wall-heat transfer between laminar and turbulent fields depends on the turbulence model used. When Ra is varied, the literature often refers to laminar and turbulent “branches” of solutions as Ra passes a critical value. When a turbulence model is included, the solution

can depart from the laminar branch for $\text{Ra} > \text{Ra}_c$ and follows the turbulent branch: Ra_c in this analysis is called separation point of the governing equations.

The Rayleigh number is calculated as in the clear fluid case. It is important to emphasize that the present results were started with the solution for the cavity without the porous obstruction and $\text{Ra}=4 \times 10^4$, Fig. 2, which has a remarkable plume impinging at the center of the cavity. It is known that the solutions for vertical cavities are not unique, but, the bifurcation of the solution is out of the concern of this work.

Figures 3–5 show the streamlines, isotherms, and isolines of turbulent kinetic energy for turbulent flow in a vertical square cavity with a porous obstruction at its midheight for Ra ranging from 4×10^4 to 10^7 . For lower values of Ra, not shown here, the isotherms are stratified and the main mechanism of heat transfer is conduction and the generation of turbulent kinetic energy is null due to the low velocity gradients.

For $\text{Ra}=4 \times 10^4$, a plume arise from the bottom of the heated wall impinging through the porous obstruction, Fig. 4(a). The flow is divided in two vortices of each side of the porous obstruction, Fig. 3(a). The generation of turbulent kinetic energy remains small and it is almost null everywhere, Fig. 5(a).

Increasing Ra to 10^6 , the plume becomes stronger, impinging through the porous obstruction more intensively, Fig. 4(b). The vortices move a little faster than before, Fig. 3(b), and the generation of turbulent kinetic energy is now evident, mainly inside and around the vicinity of the porous obstruction (Fig. 5(b)). As proposed by Ref. [29], the porous matrix contributes with the generation of turbulent kinetic energy such that a new term G^i in the $\langle k \rangle^i$ transport equation (14) was introduced. For a fixed value of the Darcy velocity through a porous bed, the amount of mechanical energy converted into turbulence should depend on the medium properties. For the limiting case of high porosity and permeability media ($\phi \rightarrow 1 \Rightarrow K \rightarrow \infty$) no fraction of this available mechanical energy is expected to generate turbulence. The flow, in this situation, behaves like clear fluid flow. As the flow resistance increases, by increasing ϕ/\sqrt{K} , gradients of local u within the pore will contribute to increasing $\langle k \rangle^i$. This porous obstruction, as will be shown later, forces an earlier departure of Nu calculated for both regimes, namely, laminar and turbulent.

For $\text{Ra}=10^7$, two plumes arise from the porous obstruction of each side of the square cavity. Both plumes point to opposing directions and move toward to the heated walls, Fig. 4(c). This feature makes the streamlines, Fig. 3(c), change its directions, probably to minimize the shear stresses between the vortices. Therefore, the isolines of turbulent kinetic energy are very pronounced in the porous matrix and present symmetry with respect to the center of the cavity, Fig. 5(c).

Table 1 shows the Nusselt numbers for a vertical square cavity with two possibilities: (a) vertical square cavity with a porous obstruction and (b) vertical square cavity without a porous obstruction. It is interesting to note that for clear cavities (unobstructed flow) the values of Nu calculated with and without the turbulence model shows nearly the same values (cases (b) in Table 1). As mentioned above, this is an indication that within the selected range for Ra, namely $10^2 < \text{Ra} < 10^7$, turbulence seems to be not yet fully established in an “empty” cavity. An increase in k within the flow has to be “promoted” by some sort of agent, similarly to what happens when an orderly laminar flow is forced through a “grid,” generating turbulence by disturbing the flow past the solid wires.

Further, Table 1 clearly shows that the overall values of the Nusselt number for a vertical square cavity without a porous obstruction are higher than those with porous obstruction (cases (a) and (b) in Table 1). The porous plate damps the heat transfer across the heated walls, showing an overall lower Nusselt numbers, for each Ra, when compared with those without porous obstruction.

Also, when the two solutions are compared for the cases with

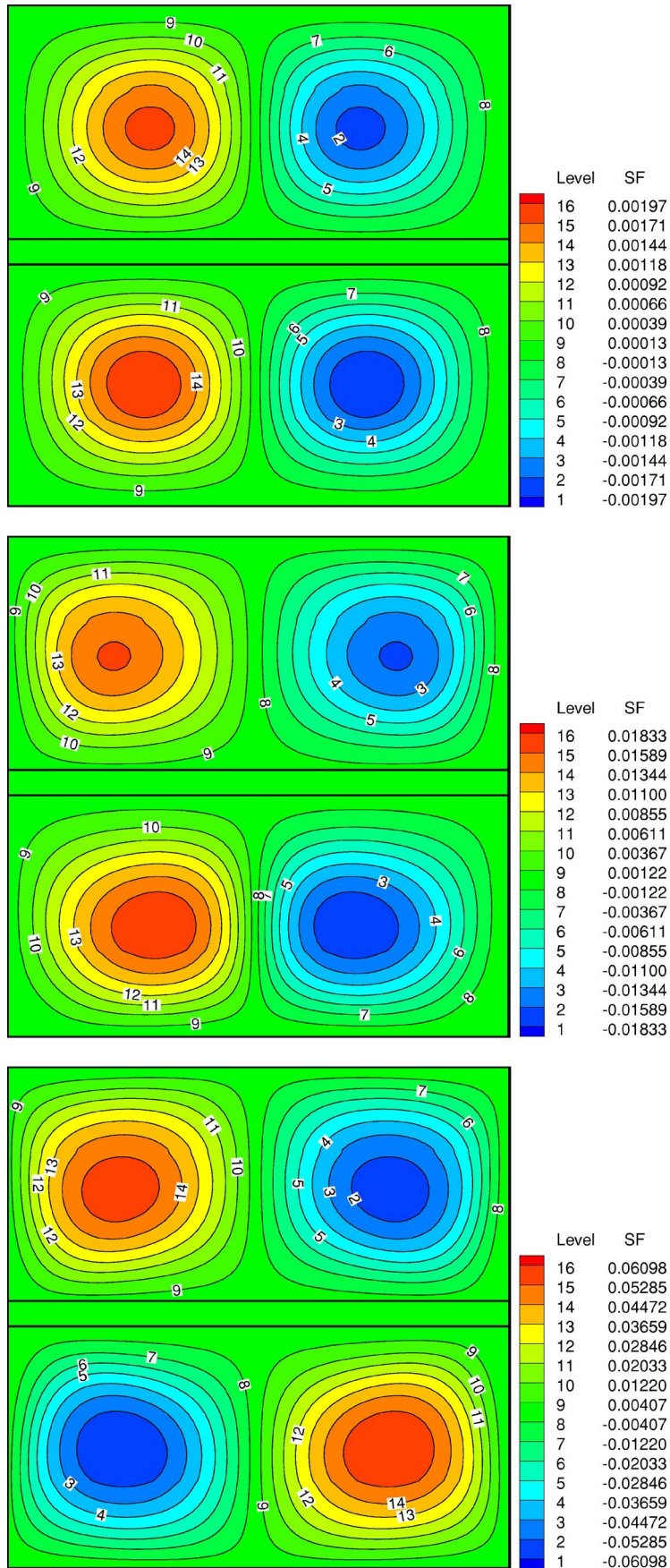
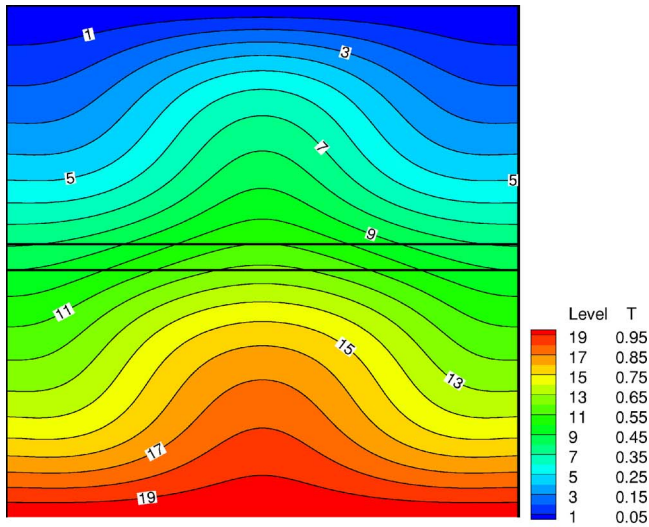
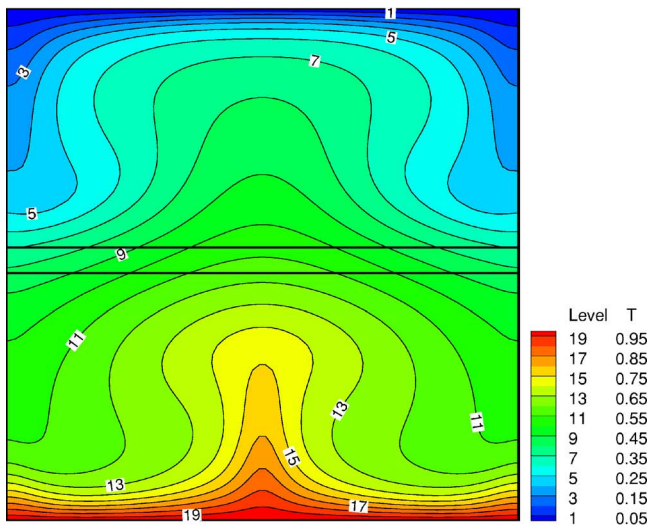


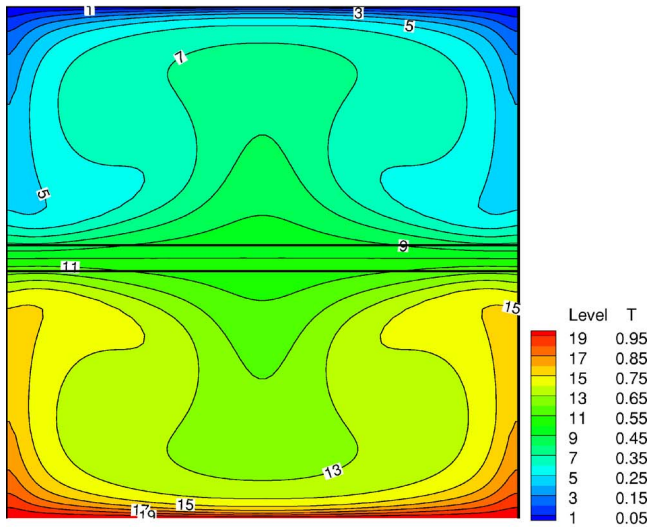
Fig. 3 Streamlines of turbulent solution of a vertical square cavity with a porous obstruction for $Ra=4 \times 10^4$, 10^6 , and 10^7 with $\phi=0.95$ and $D_p = 1$ mm



(a)



(b)



(c)

Fig. 4 Isotherms of turbulent solution of a vertical square cavity with a porous obstruction for (a) $Ra=4 \times 10^4$, (b) 10^6 , and (c) 10^7 with $\phi=0.95$ and $D_p=1$ mm

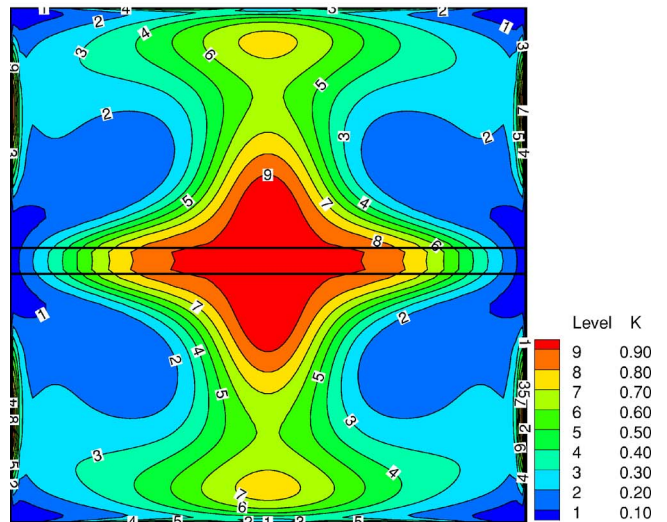
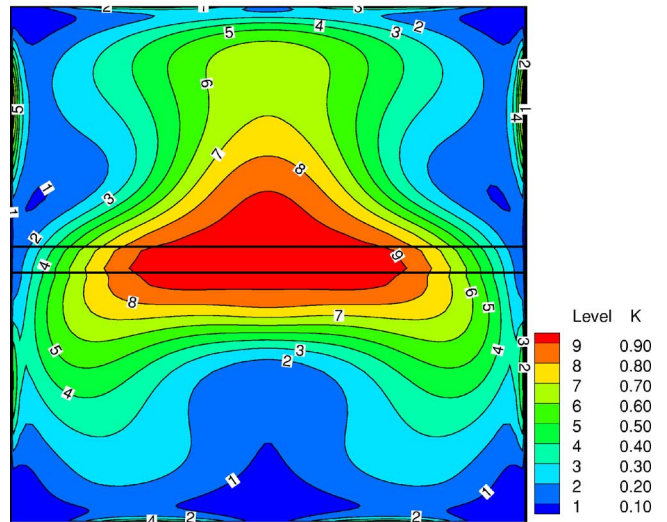
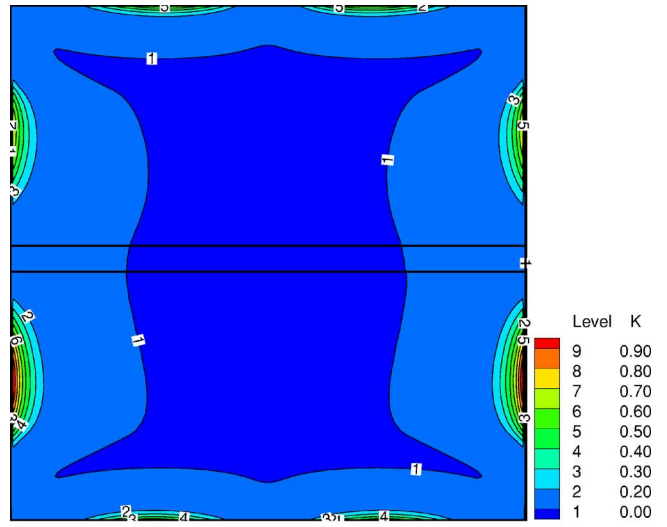


Fig. 5 Isolines of k for turbulent solution for a vertical square cavity with a porous obstruction for $Ra=4 \times 10^4$, 10^6 , and 10^7 with $\phi=0.95$ and $D_p=1$ mm

the porous plate (cases (a) in Table 1), even for a relatively low Ra number, $Ra < 10^7$, the turbulent model solution differs by a considerably amount from the laminar one. For example, for Ra

Table 1 Average Nusselt numbers for $10^2 < Ra < 10^7$ with $\phi = 0.95$ and $D_p = 1$ mm: (a) with porous obstruction and (b) without porous obstruction

	Ra	10^2	4×10^4	10^6	10^7
Laminar solution	a	1.00	1.32	3.79	7.05
	b	1.00	2.87	6.58	11.74
Turbulent solution	a	1.00	1.32	5.44	10.83
	b	1.00	2.88	6.65	12.32

$= 10^6$ Nu is $100 \times (5.44 - 3.79) / 3.79 = 43.53\%$ higher if the turbulent model is compared with the laminar result, whereas for the clear cavity case the laminar and turbulent solutions give similar values. For $Ra = 10^7$, the inclusion of the porous plate yields an increase in Nu by $100 \times (10.83 - 7.05) / 7.05 = 53.62\%$ when turbulent and laminar models are compared. As such, the presence of a porous obstruction in the square cavity seems to force an earlier increase in Nu, and that can be interpreted as an earlier separation of the laminar branch to the turbulent branch of the solution.

7 Conclusion

This paper presented computations for laminar and turbulent flows with the standard $k-\epsilon$ model with a wall function for natural convection in a square cavity with a porous obstruction in the middle. Nusselt numbers for a vertical square cavity without a porous obstruction are higher than those with porous obstruction. The porous obstruction damps the heat transfer across the heated walls, showing an overall lower Nusselt numbers when compared with those with porous obstruction. However, the presence of a porous obstruction in the square cavity seems to force an earlier separation of the laminar branch to the turbulent branch due to the higher generation of turbulent kinetic energy in the porous matrix. Analyses of important environmental and engineering flows can benefit from the derivations herein and, ultimately, it is expected that additional research on this new subject be stimulated by the work here presented.

Acknowledgment

The authors are grateful to CNPq and FAPESP, Brazil, for their financial support during the course of this research.

Nomenclature

Latin Characters

- c_F = Forchheimer coefficient
- $c_{1,2,3,k,\mu}$ = model constants
- c_p = fluid specific heat, $J/kg^\circ C$
- Da = Darcy number, $Da = K/L^2$
- \mathbf{g} = gravity acceleration vector, m/s^2
- H = square height, m
- K = permeability, $K = D_p^2 \phi^3 / 144(1 - \phi)^2$, m^2
- k = turbulent kinetic energy, J/kg
- k_f = fluid thermal conductivity, $W/m^\circ C$
- k_s = solid thermal conductivity, $W/m^\circ C$
- L = square width
- Nu = $Nu = hH/k$, Nusselt number
- Ra = $Ra = g\beta H^3 \Delta T / \nu \alpha$, fluid Rayleigh number
- T = Temperature, $^\circ C$
- \mathbf{u} = microscopic velocity, m/s
- \mathbf{u}_D = Darcy or superficial velocity (volume average of \mathbf{u})

Greek Characters

- α = fluid thermal diffusivity, m^2/s
- β = fluid thermal expansion coefficient, $1/^\circ K$

- ΔV = representative elementary volume, m^2
- ΔV_f = fluid volume inside ΔV
- ϵ = dissipation rate ϵ , W/kg
- μ = fluid dynamic viscosity, $N \cdot s/m^2$
- $\mu_{t,\phi}$ = macroscopic turbulent viscosity, $N \cdot s/m^2$
- ν = fluid kinematic viscosity, m^2/s
- ρ = fluid density, kg/m^3
- $\sigma_{k,\epsilon,T}$ = turbulence model constants
- $\phi = \phi = \Delta V_f / \Delta V$, porosity

Special Characters

- φ = general variable
- $\bar{\varphi}$ = temporal average
- φ' = temporal fluctuation
- $\langle \varphi \rangle^i$ = intrinsic average
- $\langle \varphi \rangle^v$ = volume average
- ${}^i \varphi$ = spatial deviation
- φ = vectorial general variable
- $\varphi_{s,f}$ = solid/fluid
- $\phi_{H,C}$ = hot/cold
- $()^T$ = transpose

References

- [1] Jones, I. P., 1979, *A Comparison Problem for Numerical Methods in Fluid Dynamics: The Double-Glazing Problem*, *Numerical Methods in Thermal Problems*, R. W. Lewis and K. Morgan, eds., Pineridge Press, Swansea, pp. 338–348.
- [2] de Vahl Davis, G., 1983, "Natural Convection in a Square Cavity: A Benchmark Numerical Solution," *Int. J. Numer. Methods Fluids*, **3**, pp. 249–264.
- [3] de Vahl Davis, G., and Jones, I. P., 1983, "Natural Convection in a Square Cavity—A Comparison Exercise," *Int. J. Numer. Methods Fluids*, **3**, pp. 227–248.
- [4] Markatos, N. C., and Pericleous, K. A., 1984, "Laminar and Turbulent Natural Convection in an Enclosed Cavity," *Int. J. Heat Mass Transfer*, **27**, pp. 755–772.
- [5] Henkes, R. A. W. M., van der Vlugt, F. F., and Hoogendoorn, C. J., 1991, "Natural-Convection Flow in a Square Cavity Calculated With Low-Reynolds-Number Turbulence Models," *Int. J. Heat Mass Transfer*, **34**(2), pp. 377–388.
- [6] Fusegi, T., Hyun, J. M., and Kuwahara, K., 1991, "Three-Dimensional Simulations of Natural Convection in a Sidewall-Heated Cube," *Int. J. Numer. Methods Fluids*, **3**, pp. 857–867.
- [7] Barakos, G., Mitsoulis, E., and Assimacopoulos, D., 1994, "Natural Convection Flow in a Square Cavity Revised: Laminar and Turbulent Models With Wall Function," *Int. J. Numer. Methods Fluids*, **18**, pp. 695–719.
- [8] Nield, D. A., and Bejan, A., 1992, *Convection in Porous Media*, Springer, New York.
- [9] Ingham, D. B., and Pop, I., 1998, *Transport Phenomena in Porous Media*, Elsevier, Amsterdam.
- [10] Walker, K. L., and Homsy, G. M., 1978, "Convection in Porous Cavity," *J. Fluid Mech.*, **87**, pp. 449–474.
- [11] Bejan, A., 1979, "On the Boundary Layer Regime in a Vertical Enclosure Filled With a Porous Medium," *Lett. Heat Mass Transfer*, **6**, pp. 93–102.
- [12] Prasad, V., and Kulacki, F. A., 1984, "Convective Heat Transfer in a Rectangular Porous Cavity—Effect of Aspect Ratio on Flow Structure and Heat Transfer," *ASME J. Heat Transfer*, **106**, pp. 158–165.
- [13] Beckermann, C., Viskanta, R., and Ramadhyani, S., 1986, "A Numerical Study of Non-Darcian Natural Convection in a Vertical Enclosure Filled With a Porous Medium," *Numer. Heat Transfer*, **10**, pp. 557–570.
- [14] Gross, R. J., Bear, M. R., and Hickox, C. E., 1986, "The Application of Flux-Corrected Transport (Fct) to High Rayleigh Number Natural Convection in a Porous Medium," *Proc. 8th Int. Heat Transfer Conf.*, San Francisco, CA.
- [15] Manole, D. M., and Lage, J. L., 1992, "Numerical Benchmark Results for Natural Convection in a Porous Medium Cavity, Heat and Mass Transfer in Porous Media," *Asme Conference, Htd*, **216**, pp. 55–60.
- [16] Baytas, A. C., and Pop, I., 1999, "Free Convection in Oblique Enclosures Filled With a Porous Medium," *Int. J. Heat Mass Transfer*, **42**, pp. 1047–1057.
- [17] Hsu, C. T., and Cheng, P., 1990, "Thermal Dispersion in a Porous Medium," *Int. J. Heat Mass Transfer*, **33**, pp. 1587–1597.
- [18] Bear, J., 1972, *Dynamics of Fluids in Porous Media*, American Elsevier, New York.
- [19] Whitaker, S., 1966, "Equations of Motion in Porous Media," *Chem. Eng. Sci.*, **21**, pp. 291–300.
- [20] Whitaker, S., 1967, "Diffusion and Dispersion in Porous Media," *Am. Inst. Chem. Eng. Symp. Ser.*, **13**(3), pp. 420–427.
- [21] Masuoka, T., and Takatsu, Y., 1996, "Turbulence Model for Flow Through Porous Media," *Int. J. Heat Mass Transfer*, **39**(13), pp. 2803–2809.
- [22] Kuwahara, F., Nakayama, A., and Koyama, H., 1996, "A Numerical Study of Thermal Dispersion in Porous Media," *ASME J. Heat Transfer*, **118**, pp. 756–761.

- [23] Kuwahara, F., and Nakayama, A., 1998, "Numerical Modeling of Non-Darcy Convective Flow in a Porous Medium," *Heat Transfer 1998: Proceedings. 11th Int. Heat Transf. Conf., Kyongyu, Korea*, Taylor & Francis, Washington, D. C., Vol. 4, pp. 411–416.
- [24] Nakayama, A., and Kuwahara, F., 1999, "A Macroscopic Turbulence Model for Flow in a Porous Medium," *ASME J. Fluids Eng.*, **121**, pp. 427–433.
- [25] Lee, K., and Howell, J. R., 1987, "Forced Convective and Radiative Transfer Within a Highly Porous Layer Exposed to a Turbulent External Flow Field," *Proceedings of the 1987 ASME-JSME Thermal Engineering Joint Conf., Honolulu, Hawaii*, ASME, New York, Vol. 2, pp. 377–386.
- [26] Antohe, B. V., and Lage, J. L., 1997, "A General Two-Equation Macroscopic Turbulence Model for Incompressible Flow in Porous Media," *Int. J. Heat Mass Transfer*, **40**(13), pp. 3013–3024.
- [27] Getachewa, D., Minkowycz, W. J., and Lage, J. L., 2000, "A Modified Form of the k - ϵ Model for Turbulent Flow of an Incompressible Fluid in Porous Media," *Int. J. Heat Mass Transfer*, **43**, pp. 2909–2915.
- [28] Pedras, M. H. J., and de Lemos, M. J. S., 2000, "On the Definition of Turbulent Kinetic Energy for Flow in Porous Media," *Int. Commun. Heat Mass Transfer*, **27**(2), pp. 211–220.
- [29] Pedras, M. H. J., and de Lemos, M. J. S., 2001, "Macroscopic Turbulence Modeling for Incompressible Flow Through Undeformable Porous Media," *Int. J. Heat Mass Transfer*, **44**(6), pp. 1081–1093.
- [30] Pedras, M. H. J., and de Lemos, M. J. S., 2001, "Simulation of Turbulent Flow in Porous Media Using a Spatially Periodic Array and a Low-Re Two-Equation Closure," *Numer. Heat Transfer, Part A*, **39**(1), pp. 35–59.
- [31] Pedras, M. H. J., and de Lemos, M. J. S., 2001, "On the Mathematical Description and Simulation of Turbulent Flow in a Porous Medium Formed by an Array of Elliptic Rods," *ASME J. Fluids Eng.*, **123**(4), pp. 941–947.
- [32] Rocamora, F. D., Jr., and de Lemos, M. J. S., 2000, "Analysis of Convective Heat Transfer of Turbulent Flow in Saturated Porous Media," *Int. Commun. Heat Mass Transfer*, **27**(6), pp. 825–834.
- [33] de Lemos, M. J. S., and Rocamora, F. D., 2002, "Turbulent Transport Modeling for Heated Flow in Rigid Porous Media," *Proceedings of the Twelfth International Heat Transfer Conference*, Grenoble, France, August 18–23, pp. 791–795.
- [34] de Lemos, M. J. S., and Braga, E. J., 2003, "Modeling of Turbulent Natural Convection in Saturated Rigid Porous Media," *Int. Commun. Heat Mass Transfer*, **30**(5), pp. 615–624.
- [35] Braga, E. J., and de Lemos, M. J. S., 2004, "Turbulent Natural Convection in a Porous Square Cavity Computed With a Macroscopic k - ϵ Model," *Int. J. Heat Mass Transfer*, **47**, pp. 5639–5650.
- [36] Saito, M., and de Lemos, M. J. S., 2005, "Interfacial Heat Transfer Coefficient for Non-Equilibrium Convective Transport in Porous Media," *Int. Commun. Heat Mass Transfer*, **32**(5), pp. 667–677.
- [37] Saito, M., and de Lemos, M. J. S., 2006, "A Correlation for Interfacial Heat Transfer Coefficient for Turbulent Flow Over an Array of Square Rods," *ASME J. Heat Transfer*, **128**(5), pp. 444–452.
- [38] de Lemos, M. J. S., and Mesquita, M. S., 2003, "Turbulent Mass Transport in Saturated Rigid Porous Media," *Int. Commun. Heat Mass Transfer*, **30**(1), pp. 105–113.
- [39] de Lemos, M. J. S., and Tofaneli, L. A., 2004, "Modeling of Double-Diffusive Turbulent Natural Convection in Porous Media," *Int. J. Heat Mass Transfer*, **47**(19–20), pp. 4221–4231.
- [40] Assato, M., Pedras, M. H. J., and de Lemos, M. J. S., 2005, "Numerical Solution of Turbulent Channel Flow Past a Backward-Facing Step With a Porous Insert Using Linear and Nonlinear k - ϵ Models," *J. Porous Media*, **8**(1), pp. 13–29.
- [41] Santos, N. B., and de Lemos, M. J. S., 2006, "Flow and Heat Transfer in a Parallel Plate Channel With Porous and Solid Baffles," *Numer. Heat Transfer, Part A*, **49**(5), pp. 471–494.
- [42] Silva, R. A., and de Lemos, M. J. S., 2003, "Numerical Analysis of the Stress Jump Interface Condition for Laminar Flow Over a Porous Layer," *Numer. Heat Transfer, Part A*, **43**(6), pp. 603–617.
- [43] Silva, R. A., and de Lemos, M. J. S., 2003, "Turbulent Flow in a Channel Occupied by a Porous Layer Considering the Stress Jump at the Interface," *Int. J. Heat Mass Transfer*, **46**, pp. 5113–5121.
- [44] de Lemos, M. J. S., 2005, "Turbulent Kinetic Energy Distribution Across the Interface Between a Porous Medium and a Clear Region," *Int. Commun. Heat Mass Transfer*, **32**(1–2), pp. 107–115.
- [45] de Lemos, M. J. S., and Silva, R. A., 2006, "Turbulent Flow Over a Layer of a Highly Permeable Medium Simulated With a Diffusion-Jump Model for the Interface," *Int. J. Heat Mass Transfer*, **49**(3–4), pp. 546–556.
- [46] de Lemos, M. J. S., and Pedras, M. H. J., 2001, "Recent Mathematical Models for Turbulent Flow for Saturated Rigid Porous Media," *ASME J. Fluids Eng.*, **123**(4), pp. 935–940.
- [47] de Lemos, M. J. S., 2006, *Turbulence in Porous Media: Modeling and Applications*, Elsevier, New York.
- [48] Kuwahara, F., Kameyama, Y., Yamashita, S., and Nakayama, A., 1998, "Numerical Modeling of Turbulent Flow in Porous Media Using a Spatially Periodic Array," *J. Porous Media*, **1**(1), pp. 47–55.
- [49] Ergun, S., 1952, "Fluid Flow Through Packed Columns," *Chem. Eng. Process.*, **48**, pp. 89–94.
- [50] Ochoa-Tapia, J. A., and Whitaker, S., 1995, "Momentum Transfer at the Boundary Between a Porous Medium and a Homogeneous Fluid—I. Theoretical Development," *Int. J. Heat Mass Transfer*, **38**, pp. 2635–2646.
- [51] Lee, K., and Howell, J. R., 1987, "Forced Convective and Radiative Transfer Within a Highly Porous Layer Exposed to a Turbulent External Flow Field," *Proceedings Of The 1987 ASME-JSME Thermal Engineering Joint Conf.*, Vol. 2, pp. 377–386.
- [52] Khosla, P. K., and Rubin, S. G., 1974, "A Diagonally Dominant Second-Order Accurate Implicit Scheme," *Comput. Fluids*, **2**, pp. 207–209.
- [53] Patankar, S. V., and Spalding, D. B., 1972, "A Calculation Procedure for Heat, Mass and Momentum Transfer in Three Dimensional Parabolic Flows," *Int. J. Heat Mass Transfer*, **15**, pp. 1787–1806.
- [54] Stone, H. L., 1968, "Iterative Solution of Implicit Approximations of Multi-Dimensional Partial Differential Equations," *SIAM (Soc. Ind. Appl. Math.) J. Numer. Anal.*, **5**, pp. 530–558.
- [55] Ozoe, H., Mouri, A., Ohmuro, M., Churchill, S. W., and Lior, N., 1985, "Numerical Calculations of Laminar and Turbulent Natural Convection in Water in Rectangular Channels Heated and Cooled Isothermally on the Opposing Vertical Walls," *Int. J. Heat Mass Transfer*, **28**, pp. 125–138.